PAPER

Tension-controlled single-crystallization of copper foils for roll-to-roll synthesis of high-quality graphene films

2D Materials

RECEIVED
12 September 2017

REVISED
17 November 2017

ACCEPTED FOR PUBLICATION
15 January 2018

PUBLISHED
1 February 2018

PAPER

Tension-controlled single-crystallization of copper foils for roll-to-roll synthesis of high-quality graphene films

Insu Jo[1,9], Subeom Park[1,9], Dongjin Kim[2], Jin San Moon[3], Won Bae Park[3], Tae Hyeong Kim[3], Jin Hyoun Kang[4], Wonbae Lee[5], Youngsoo Kim[5], Dong Nyung Lee[6], Sung-Pyo Cho[7], Hyunchul Choi[8], Inbyeong Kang[8], Jong Hyun Park[8], Jeong Soo Lee[3] and Byung Hee Hong[1,2,5]

[1] Advanced Institute of Convergence Technology and Department of Chemistry, Graphene Research Center, Seoul National University, Seoul 08826, Republic of Korea
[2] Program in Nano Science and Technology, Graduate School of Convergence Science and Technology, Seoul National University, Seoul 08826, Republic of Korea
[3] Advanced Materials Team, Materials and Production Engineering Research Institute, LG Electronics, Seoul 06763, Republic of Korea
[4] Department of Physics and Astronomy, Institute of Applied Physics, Seoul National University, Seoul 08826, Republic of Korea
[5] Graphene Square Inc., Inter-University Semiconductor Research Center, Seoul National University, Seoul 08826, Republic of Korea
[6] Department of Materials Science and Engineering, Seoul National University, Seoul 08826, Republic of Korea
[7] National Center for Inter-University Research Facilities, Seoul National University, Seoul 08826, Republic of Korea
[8] LG Display, Paju-Si, Gyeonggi-Do, 10485, Republic of Korea
[9] These authors contributed equally to this work.

E-mail: byunghee@snu.ac.kr, jeongsoo.lee@lge.com and jhparkjh@lgdisplay.com

Keywords: tension, single-crystal, high-quality, graphene

Abstract

It has been known that the crystalline orientation of Cu substrates plays a crucial role in chemical vapor deposition (CVD) synthesis of high-quality graphene. In particular, Cu (1 1 1) surface showing the minimum lattice mismatch with graphene is expected to provide an ideal catalytic reactivity that can minimize the formation of defects, which also induces larger single-crystalline domain sizes of graphene. Usually, the Cu (1 1 1) substrates can be epitaxially grown on single-crystalline inorganic substrates or can be recrystallized by annealing for more than 12 h, which limits the cost and time-effective synthesis of graphene. Here, we demonstrate a new method to optimize the crystalline orientations of vertically suspended Cu foils by tension control during graphene growth, resulting in large-area recrystallization into Cu (1 1 1) surface as the applied tension activates the grain boundary energy of Cu and promotes its abnormal grain growth to single crystals. In addition, we found a clue that the formation of graphene cooperatively assists the recrystallization into Cu (1 1 1) by minimizing the surface energy of Cu. The domain sizes and charge carrier mobility of graphene grown on the single-crystalline Cu (1 1 1) are 5 times and ~50% increased, respectively, in comparison with those of graphene from Cu (1 0 0), indicating that the less lattice mismatch and the lower interaction energy between Cu (1 1 1) and graphene allows the growth of larger single-crystalline graphene with higher charge carrier mobility. Thus, we believe that our finding provides a crucial idea to design a roll-to-roll (R2R) graphene synthesis system where the tension control is inevitably involved, which would be of great importance for the continuous production of high-quality graphene in the future.

Graphene can be synthesized by chemical vapor deposition (CVD) on diverse metal catalysts such as Ir [1], Ni [2], Ru [3], Fe [4], and Cu [5–8]. Among them, Cu has been regarded as the most promising catalytic substrate owing to its lower cost and suitable carbon solubility that suppresses the growth of multilayers [9]. However, the electrical properties of the CVD-grown graphene are not as good as those of exfoliated graphene because of its polycrystallinity and grain boundary originated from the randomly oriented nucleation and growth of graphene islands [10, 11]. It was reported that the Cu (1 1 1) surface showing only 3–4% lattice mismatch with graphene decreases the defect density of graphene, and thus, enhances the electrical property [12]. The Cu (1 1 1) substrates were typically obtained by the deposition and annealing of thin Cu films on sapphire or SiO_2 wafers with limited size and cost [13–15]. The annealing of polycrystalline

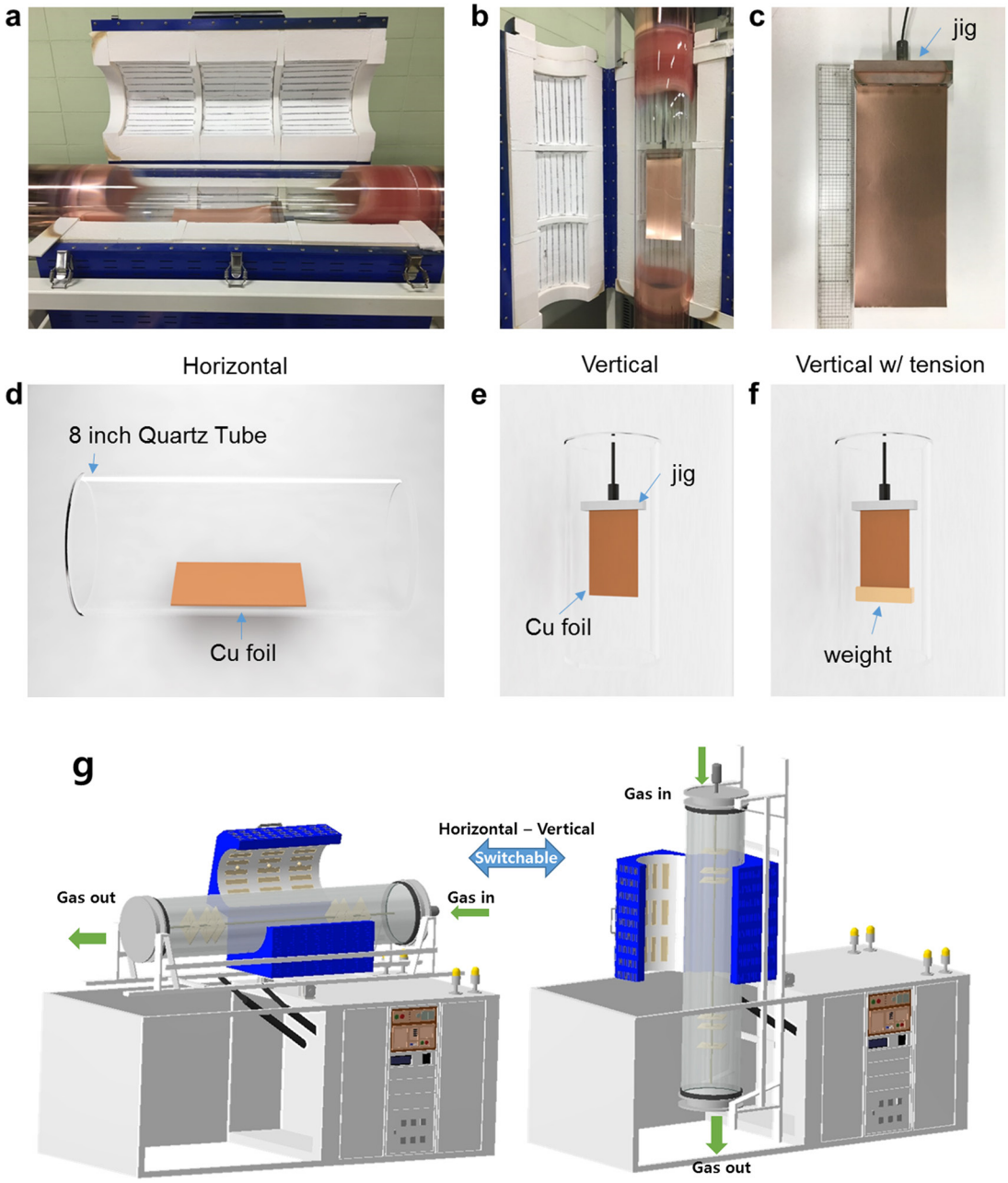

Figure 1. (a)–(c) Photographs of a horizontal–vertical switchable CVD system and a holding jig. (d) and (e) Schematic illustrations of horizontally and vertically loaded Cu foils without additional tension, respectively. (f) A schematic illustration of a vertically loaded Cu foil with tension applied by a weight. (g) An illustration of the *in situ* switchable horizontal–vertical CVD system, which provides identical growth conditions except the vertical tension by gravitation or additional weights applied to Cu foils.

Cu foils can induce the recrystallization into Cu (1 1 1), but it usually takes more than 12 h [16]. On the other hand, conventional thin copper foils are known to show Cu (1 0 0) orientation dominantly after the CVD synthesis that is typically 1–2 h long [17, 18].

The grain boundary energy is closely related to abnormal grain growth (AGG) in various metals [19–24], which can be controlled by mechanical tension. This tension-controlled recrystallization condition can be created by vertically suspending Cu foils with variable tension during the CVD synthesis of graphene. The vertical tension at ~970 °C promotes the dynamic recrystallization into small grains first and then induces secondary recrystallization into larger grains other than Cu (1 0 0), which is common orientation for cold rolled Cu foils [16]. Thus, we tried to optimize the vertical tension on the suspended Cu foils to find the recrystallization condition for Cu (1 1 1), and characterized the results after annealing only and after graphene synthesis by Raman spectroscopy, transmission electron microscopy (TEM), electron back-scattered diffraction (EBSD), x-ray diffraction (XRD), electron transport measurements, *etc*.

Figure 1 shows the photographs and illustrations of a horizontal–vertical switchable CVD setup with an 8 inch quartz tube, which provides an identical growth conditions except the vertical tension by gravitation or additional weights applied to Cu foils. Graphene was

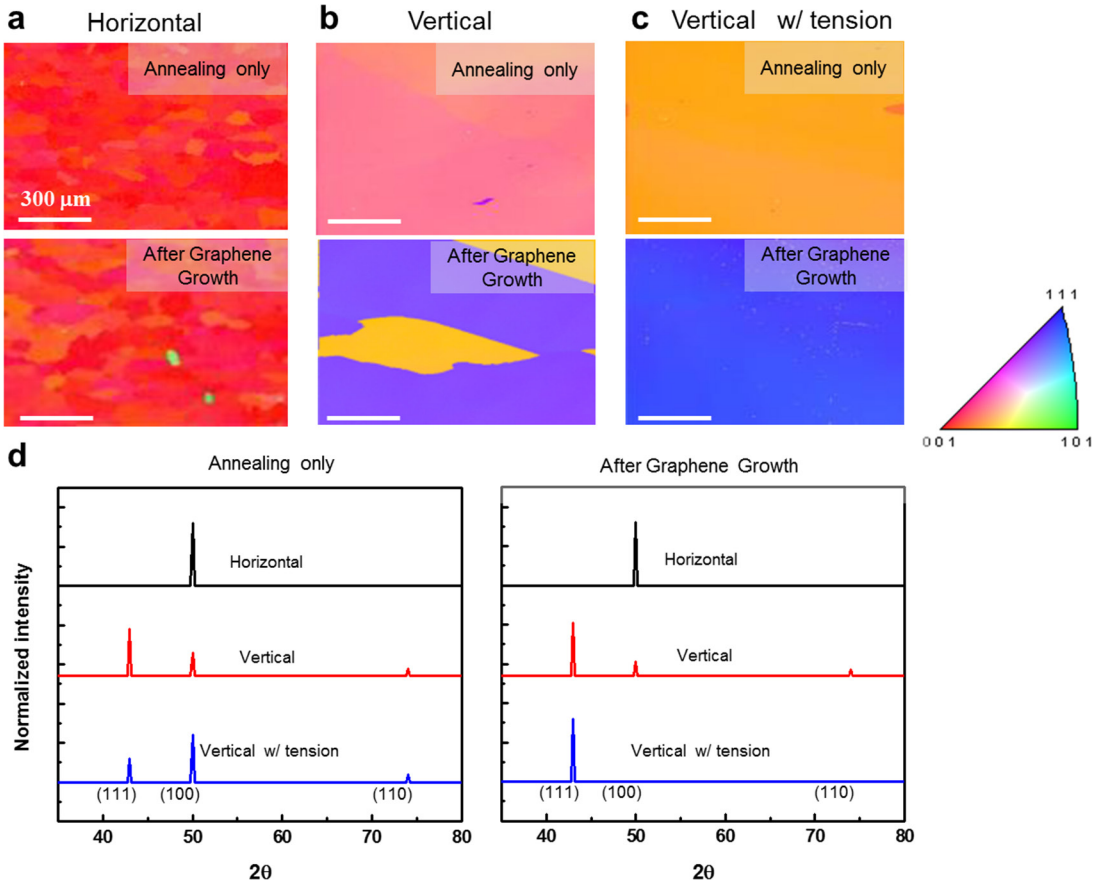

Figure 2. (a)–(c) EBSD images of annealed and graphene-grown Cu surface with horizontal/vertical geometry with/without tension control. (d) XRD spectra of annealed and graphene-grown Cu surface with and without tension control. The 2θ measured from 30° to 80° shows the three intense peaks at 43°, 50°, and 74°, which are assigned to Bragg reflections from the surface of Cu (1 1 1), (1 0 0), and (1 1 0), respectively.

synthesized using a 10 cm wide, 30 cm long, and 35 μm thick polycrystalline Cu foil (99.7%) as a catalytic substrate with flowing 50 sccm H_2 for 1 h at 970 °C under a pressure of 3.8 $\times$ 10^{-1} Torr. Next, methane was introduced into the chamber at a flow rate of 50 sccm with maintaining the chamber pressure at 8.8 $\times$ 10^{-1} Torr during the growth for 30 min. Finally, the furnace was slowly cooled down to room temperature with flowing H_2 only. For the vertical synthesis, the upper edge of the Cu foil was fixed at the holding jig (figure 1(c)) and suspended as shown in figures 1(c) and (e). The vertical tension was applied by attaching additional weight along the other edge (figure 1(f)), which were compared with the results from the horizontal growth setup (figure 1(d)).

Figures 2(a) and (b) show the EBSD analyses of the Cu foils annealed at 970 °C and the graphene-grown Cu foils that are horizontally and vertically loaded in a growth chamber, indicating that the crystallinity of Cu is relatively uncontrollable and small. It is well known that a cold rolled Cu foil usually shows (1 0 0) orientation, following the strain energy release maximization theory [18]. On the other hand, figure 2(c) shows the case of the vertically loaded Cu foils with tension induced by adding a weight at the Cu foil, exhibiting that the crystalline orientation of Cu can be controlled in large scale. The average grain sizes of the graphene-grown Cu are increased from 87.1 μm to ~2000 μm after applying the tension, which is expected to correlate with the crystalline sizes of graphene. Figure 2(d) shows the XRD patterns of the Cu corresponding to figures 2(a)–(c), indicating that the vertically loaded Cu with tension before graphene growth shows the mixture of (1 1 1) and (1 0 0) orientations, while the horizontally loaded Cu foils still exhibit (1 0 0) dominant orientation. This implies that higher mobility of (1 1 1) tilt grain boundaries than those of (1 0 0) tends to promote the partial AGG into (1 1 1) during the annealing process [25, 26]. This AGG can be promoted by applying mechanical tensions on Cu, which has been used to large scale growth of single-crystalline metals [27], but the annealed-only Cu foils do not show perfect a single crystalline surface with low index facets even with the tension applied by 30 times weight of Cu.

It is surprising that the growth of graphene dramatically catalyzes the recrystallization into (1 1 1) dominant surfaces as shown in figure 3. When the weight was increased and annealing was carried out, it was confirmed that the crystal had a near (1 1 1) when 75 kN mm^{-2} was added (figure 3(a)). However, when graphene was synthesized, a Cu(1 1 1) crystal plane was obtained at a smaller size of 25 kN mm^{-2} (figure 3(b)). The reason for this phenomenon is thought to that the formed graphene interacts with the crystal plane

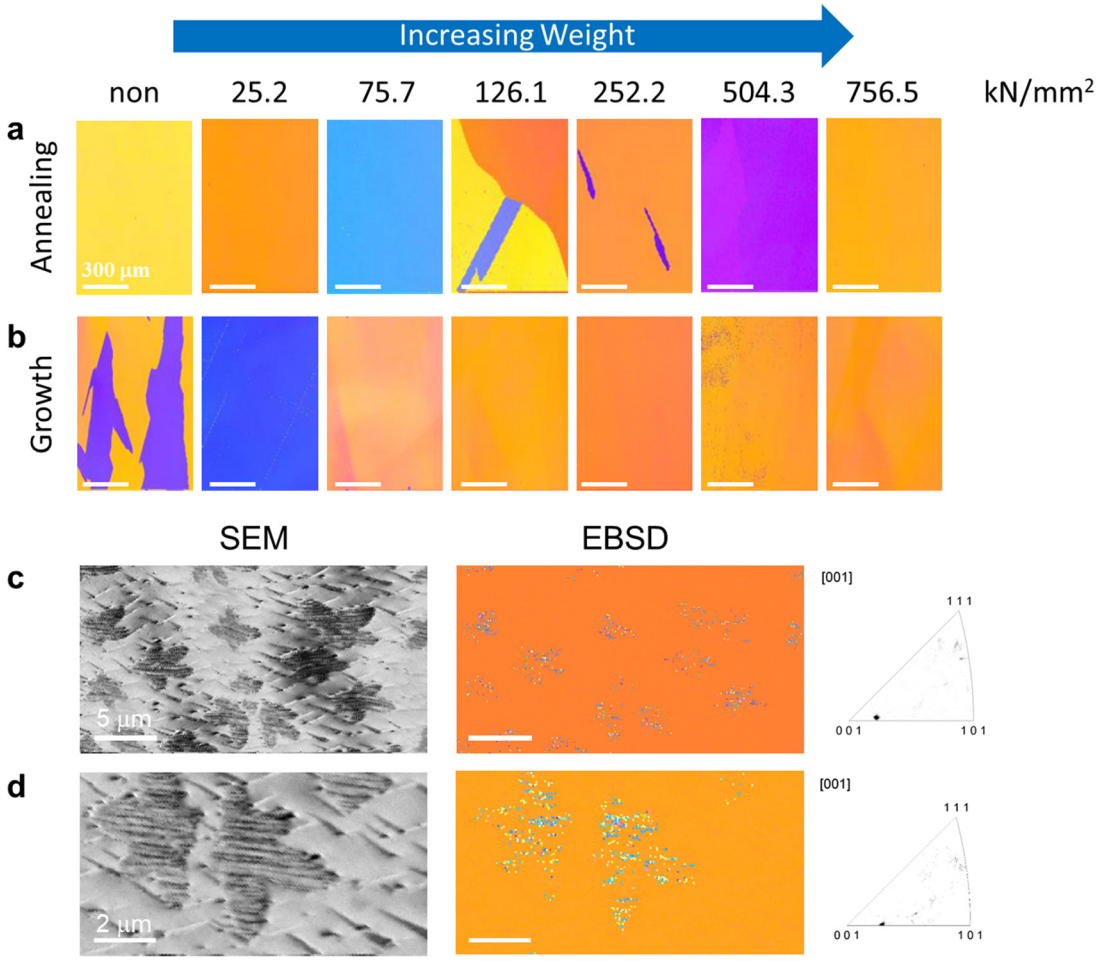

Figure 3. EBSD images of (a) annealed- and (b) graphene grown- Cu foils on a vertically loaded with increasing tension (scale bars, 300 μm). (c) and (d) SEM and EBSD images of graphene islands of Cu, indicating that the recrystallization of Cu surface can be promoted by graphene in the case of tension-controlled growth.

change to (1 1 1). The EBSD image of the graphene island after 1 min growth on the vertically loaded Cu with controlled tension clearly shows that the crystalline orientation of the graphene-covered region begins to change (figures 3(c) and (d)), while the bare Cu surface still maintains the (1 0 0) orientation. We suppose that the hexagonal lattice of graphene with a better match with Cu (1 1 1) surface than (1 0 0) results in less surface energy at the interface, promoting the crystallization into (1 1 1) cooperatively with the applied tension. Thus, the graphene-grown Cu surface with vertical tension exhibit almost (1 1 1) single-crystalline orientation at large scale as evidenced by the EBSD and XRD results in figures 2(c) and (d).

However, when strong tension is applied, the Cu (1 1 1) disappears and other mixed crystal planes appear. It has been known that the Cu texture formation is related to elastic strain energy minimization, surface energy minimization, and plastic deformation. We suppose that the strong tension applied to the Cu predominantly induces the plastic deformation, resulting in the formation of mixed crystal domains rather than a single crystal [25, 26].

It has been reported the crystallographic orientations of the catalytic substrates affect the quality as well as the growth rate of graphene film [28, 29], which is also possibly related to larger domain sizes of the graphene as the growth on Cu (1 1 1) minimizes misalignment between growing graphene islands. Thus, we carried out the grain boundary analyses of graphene by scanning diffraction mapping in TEM as shown in figures 4(a)–(c) after transferring the graphene prepared by a direct transfer method [30]. Multiple selected area electron diffractions (SAEDs) are collected as we scan the beam spots, and the positions that show the rotation of the SAEDs are marked with dots on bright-field TEM images. By repeating this process, it is possible to map the grain boundaries of graphene at much larger scale than the case of using a dark-field TEM method [10, 31]. The histograms in figures 4(a)–(c) indicate that the mean grain sizes are 4.24 ± 3.21, 3.41 ± 2.60, and 22.41 ± 15.62 μm^2 for the horizontal, vertical, and vertical Cu with tension, respectively. The result implies that there is strong correlation between the grain size of graphene and the crystalline orientation of the underlying Cu substrates, and the dynamic grain evolution can be less hindered when the growing graphene is interfaced with Cu (1 1 1) surface [32, 33].

The Raman analyses in figure 4(d) show that the 2D FWHM values are 36.8 ± 3.1, 42.4 ± 2.1,

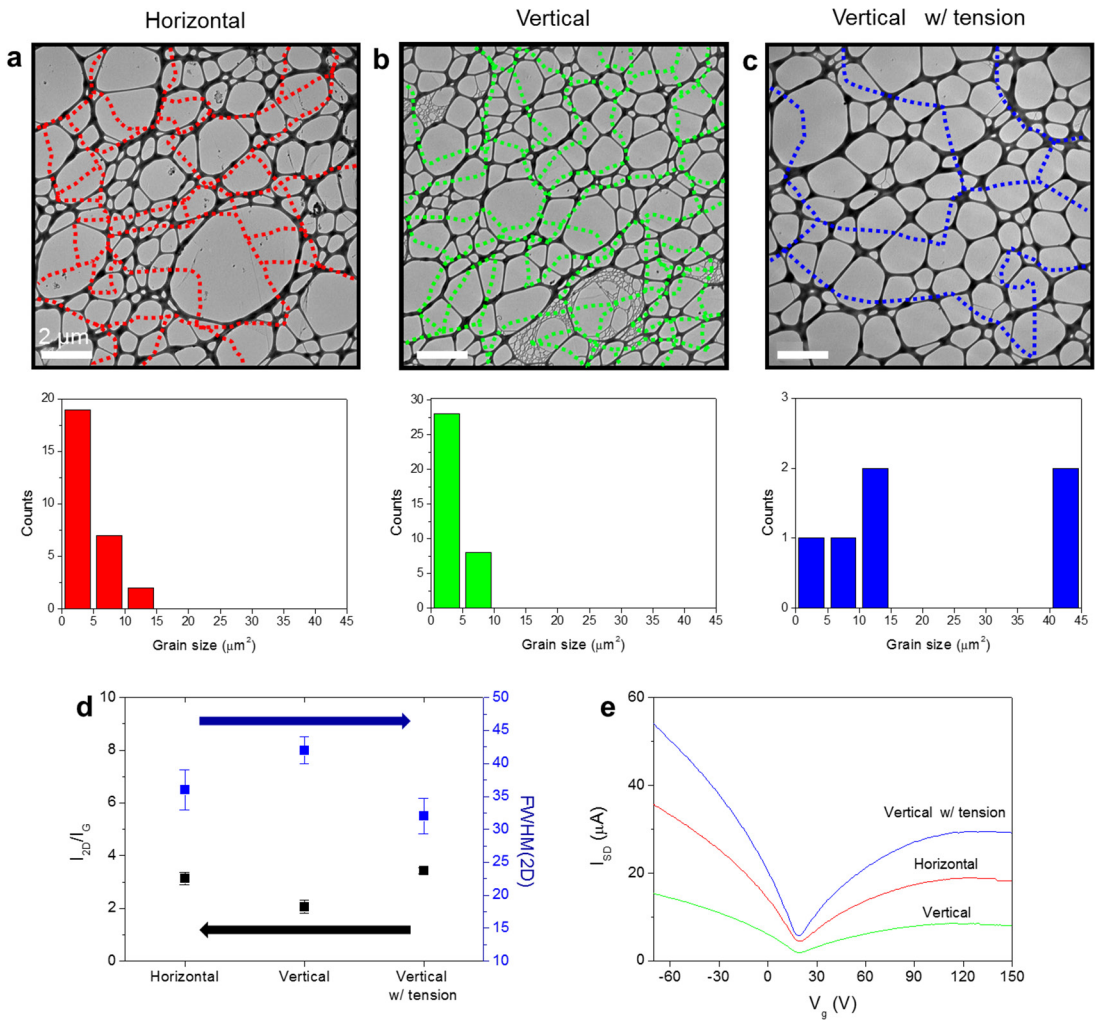

Figure 4. (a)–(c) Grain boundary analyses of graphene by scanning diffraction mapping in TEM, indicating that the graphene from vertically loaded Cu with tension (c) shows the larger domain sizes than the cases of the horizontally loaded Cu (a) and the vertically loaded Cu without additional tension (b). (d) FWHM(2D) and I(2D)/I(G) values for the Raman spectra (excitation $l = 514$ nm) of the horizontal, vertical, and vertical Cu with tension, corresponding to figures 1(d) and (e), respectively). Raman spectroscopy was performed using a 514 nm laser (e) field-effect transistor (FET) characteristics of graphene grown on the horizontal (red), vertical (green), and vertical Cu with tension (blue), showing the highest conductance and carrier mobility of the graphene grown on Cu with vertical tension.

and $32.1 \pm 2.7\,\mathrm{cm}^{-1}$, and the I(2D)/I(G) ratios are 3.1 ± 0.2, 2.0 ± 0.3, and 3.4 ± 0.1 for the graphene synthesized from the horizontal, vertical, and vertical Cu with tension, respectively. This indicates that the graphene grown on the vertically loaded Cu with tension shows the highest quality and lower doping due to the lower density of graphene boundaries [34]. The electrical properties of graphene was characterized by fabricating and measuring back-gated field-effect-transistors (FETs), where the charge carrier mobility can be determined by calculated by the following equation in the linear regime [35]:

$$I_{\mathrm{D}} = \frac{WC_i}{L} V_{\mathrm{D}} \mu (V_{\mathrm{G}} - V_{\mathrm{T}}) \qquad (1)$$

where $C_i = 1.08 \times 10^{-8}\,\mathrm{F\,cm}^{-2}$, $V_{\mathrm{D}} = 0.01\,\mathrm{V}$, $W = 230$ μm, and $L = 180$ μm. The room-temperature FET mobilities are 4376 ± 334, 2044 ± 531, and $6913 \pm 207\,\mathrm{cm}^2\,\mathrm{V}^{-1}\,\mathrm{s}^{-1}$ for the graphene synthesized from the horizontal, vertical, and vertical Cu with tension, respectively. Thus, we conclude that the (1 1 1) dominant Cu surface promotes the larger grain growth of graphene, leading to the enhanced electrical properties of graphene [36, 37].

Finally, the tension-control on the vertically loaded Cu foil has been applied to a roll-to-roll CVD system as shown in figure 5. The tension between the upper winding roll and lower unwinding roll was precisely controlled with the optimum value found in figure 3 (~25 kN mm^{-2}). The synthesis rate is as high as 300 mm min^{-1} for the stable synthesis of a 70 m long Cu foil, and temperature and gas flow ratios are the same as figure 1. The resulting graphene exhibits outstanding characteristics comparable to the graphene synthesized in the vertical CVD system, which needs to be further optimized through following studies.

In conclusion, we demonstrate a new method to optimize the crystalline orientations of vertically suspended Cu foils by tension control, resulting in large-area recrystallization into Cu (1 1 1) surface as the

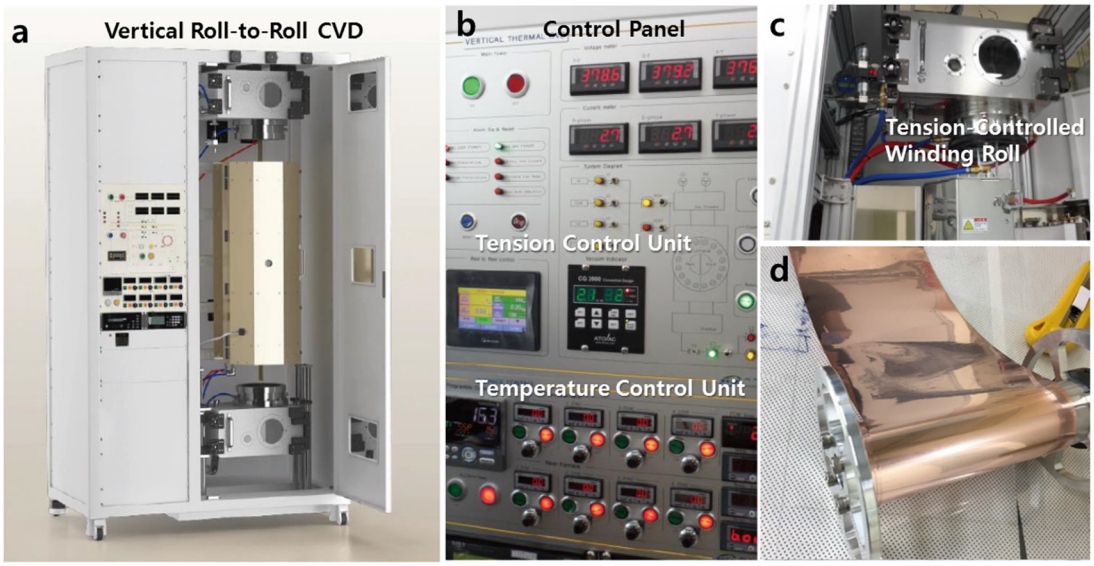

Figure 5. (a) Layout of a vertical roll-to-roll (R2R) CVD system with a tension-control unit. (b) A photograph of the control panel. (c) A photograph of the top chamber with a tension-controlled winding roll. (d) A photograph of a graphene-coated Cu roll synthesized in the tension-controlled vertical R2R system. The width and length of Cu roll was 12 cm and 70 m, respectively. The synthesis rate was 300 mm min^{-1}.

applied tension activates the grain boundary energy of Cu and promotes its AGG to single crystals as evidenced by SEM, EBSD and XRD analyses. In addition, we found a clue that the formation of graphene cooperatively assists the recrystallization into Cu (1 1 1) by minimizing the surface energy of Cu at the interface with graphene [38]. The domain sizes and electrical properties of graphene grown on the single-crystalline Cu (1 1 1) are compared with those of graphene from Cu (1 0 0), the mean graphene grain size of graphene grown on tension-controlled Cu foil (22.41 μm^2) is ~5 times larger than that from the horizontal furnace (4.24 μm^2), and the charge carrier mobility is measured to be enhanced by ~50%. This implies that the less lattice mismatch and the lower interaction energy between Cu (1 1 1) and graphene allows the growth of larger single-crystalline graphene with higher electrical quality. We believe that our finding provides a crucial idea to design a system for the CVD growth of high-quality graphene films on rolled Cu foils, where the tension control is inevitably involved, which would be of great importance for the continuous mass-production of graphene films for practical applications in the future [39–45].

Acknowledgment

This research was supported by Nano Material Technology Development Program through the National Research Foundation of Korea (NRF) funded by the Ministry of Science, ICT and Future Planning (2016M3A7B4910458) funded by the Ministry of Science, ICT, and the Industrial Strategic Technology Development Program (10079969, 10079974, 10044410) funded by the Ministry of Trade, Industry & Energy(MOTIE, Korea), and by the Inter-University Semiconductor Research Centre (ISRC) at Seoul National University.

ORCID iDs

Byung Hee Hong https://orcid.org/0000-0001-8355-8875

References

[1] Rogge P C, Thurmer K, Foster M E, McCarty K F, Dubon O D and Bartelt N C 2015 Real-time observation of epitaxial graphene domain reorientation *Nat. Commun.* **6** 6880
[2] Kim K S, Zhao Y, Jang H, Lee S Y, Kim J M, Kim K S, Ahn J H, Kim P, Choi J Y and Hong B H 2009 Large-scale pattern growth of graphene films for stretchable transparent electrodes *Nature* **457** 706–10
[3] Sutter P W, Flege J I and Sutter E A 2008 Epitaxial graphene on ruthenium *Nat. Mater.* **7** 406–11
[4] Vinogradov N A *et al* 2012 Formation and structure of graphene waves on Fe(1 1 0) *Phys. Rev. Lett.* **109** 026101
[5] Bae S *et al* 2010 Roll-to-roll production of 30-in. graphene films for transparent electrodes *Nat. Nanotechnol.* **5** 574–8
[6] Kobayashi T *et al* 2013 Production of a 100 m long high-quality graphene transparent conductive film by roll-to-roll chemical vapor deposition and transfer process *Appl. Phys. Lett.* **102** 023112
[7] Hao Y *et al* 2013 The role of surface oxygen in the growth of large single crystal graphene on copper *Science* **342** 720–3
[8] Polsen E S, McNerny D Q, Viswanath B, Pattinson S W and Hart A J 2015 High-speed roll-to-roll manufacturing of graphene using a concentric tube CVD reactor *Sci. Rep.* **5** 10257
[9] Mattevi C, Kim H and Chhowalla M 2011 A review of chemical vapour deposition of graphene on copper *J. Mater. Chem.* **21** 3324–34
[10] Huang P Y *et al* 2011 Grains and grain boundaries in single-layer graphene atomic patchwork quilts *Nature* **469** 389–92
[11] Yu Q *et al* 2011 Control and characterization of individual grains and grain boundaries in graphene grown by chemical vapour deposition *Nat. Mater.* **10** 443–9

[12] Shin H-J, Yoon S-M, Mook Choi W, Park S, Lee D, Yong Song I, Sung Woo Y and Choi J-Y 2013 Influence of Cu crystallographic orientation on electron transport in graphene *Appl. Phys. Lett.* **102** 163102
[13] Hu B, Ago H, Ito Y, Kawahara K, Tsuji M, Magome E, Sumitani K, Mizuta N, Ikeda K-I and Mizuno S 2012 Epitaxial growth of large-area single-layer graphene over Cu(1 1 1)/sapphire by atmospheric pressure CVD *Carbon* **50** 57–65
[14] Yu H K, Balasubramanian K, Kim K, Lee J-L, Maiti M, Ropers C, Krieg J, Kern K and Wodtke A M 2014 Chemical vapor deposition of graphene on a 'peeled-off' epitaxial Cu(1 1 1) foil: a simple approach to improved properties *ACS Nano* **8** 8636–43
[15] Tao L *et al* 2012 Uniform wafer-scale chemical vapor deposition of graphene on evaporated Cu (1 1 1) film with quality comparable to exfoliated monolayer *J. Phys. Chem.* C **116** 24068–74
[16] Brown L *et al* 2014 Polycrystalline graphene with single crystalline electronic structure *Nano Lett.* **14** 5706–11
[17] Gerber P, Tarasiuk J, Chauveau T and Bacroix B 2003 A quantitative analysis of the evolution of texture and stored energy during annealing of cold rolled copper *Acta Mater.* **51** 6359–71
[18] Hong S-H and Lee D N 2003 The evolution of the cube recrystallization texture in cold rolled copper sheets *Mater. Sci. Eng.* A **351** 133–47
[19] Mortazavi N, Bonora N, Ruggiero A and Hörnqvist Colliander M 2016 Dynamic recrystallization during high-strain-rate tension of copper *Metall. Mater. Trans.* A **47** 2555–9
[20] Chun H, Na S-M, Mudivarthi C and Flatau A B 2010 The role of misorientation and coincident site lattice boundaries in goss-textured galfenol rolled sheet *J. Appl. Phys.* **107** 09A960
[21] Chun H, Na S-M, Yoo J-H, Wuttig M and Flatau A B 2011 Tension and strain annealing for abnormal grain growth in magnetostrictive galfenol rolled sheet *J. Appl. Phys.* **109** 07A941
[22] Worthington D L, Pedrazas N A, Noell P J and Taleff E M 2013 Dynamic abnormal grain growth in molybdenum *Metall. Mater. Trans.* A **44** 5025–38
[23] Chang J-K, Takata K, Ichitani K and Taleff E M 2010 Abnormal grain growth and recrystallization in Al–Mg alloy AA5182 following hot deformation *Metall. Mater. Trans.* A **41** 1942–53
[24] Wang X-J *et al* 2015 Direct observation of graphene growth and associated copper substrate dynamics by *in situ* scanning electron microsocpy *ACS Nano* **5** 2142–6
[25] Park H and Lee D N 2003 The evolution of annealing textures in 90 Pct drawn copper wire *Metall. Mater. Trans.* A **34** 531
[26] Lee S B, Kim D-I, Hong S-H and Lee D N 2012 Texture evolution of abnormal grains with post-deposition annealing temperature in nanocrystalline Cu thin films *Metall. Mater. Trans.* A **44** 152–62
[27] Taleff E M and Pedrazas N A 2013 A new route for growing large grains in metals *Science* **341** 1461
[28] Wood J D, Schmucker S W, Lyons A S, Pop E and Lyding J W 2011 Effects of polycrystalline Cu substrate on graphene growth by chemical vapor deposition *Nano Lett.* **11** 4547–54
[29] Rogge P C, Nie S; McCarty K F, Bartelt N C and Dubon O D 2015 Orientation-dependent growth mechanisms of graphene Islands on Ir(1 1 1) *Nano Lett.* **15** 170–5
[30] Regan W, Alem N, Alemán B, Geng B, Girit C, Maserati L, Wang F, Crommie M and Zettl A 2010 A direct transfer of layer-area graphene *Appl. Phys. Lett.* **96** 113102
[31] Kim K, Lee Z, Regan W, Kisielowski C, Crommie M F and Zettl A 2011 Grain boundary mapping in polycrystalline graphene *ACS Nano* **5** 2142–6
[32] Vollmer S, Witte G and Wöll C 2001 Determination of site specific adsorption energies of CO on copper *Catal. Lett.* **77** 97–101
[33] Wu Y, Hao Y, Jeong H Y, Lee Z, Chen S, Jiang W, Wu Q, Piner R D, Kang J and Ruoff R S 2013 Crystal structure evolution of individual graphene Islands during CVD growth on copper foil *Adv. Mater.* **25** 6744–51
[34] Cançado L G, Jorio A and Pimenta M A 2007 Measuring the absolute Raman cross section of nanographites as a function of laser energy and crystallite size *Phys. Rev.* B **76** 064304
[35] Jo I, Kim Y, Moon J, Park S, Moon J S, Park W B, Lee J S and Hong B H 2015 Stable n-type doping of graphene via high-molecular-weight ethylene amines *Phys. Chem. Chem. Phys.* **17** 29492–5
[36] Dinh V T, Kotakoski J, Louvet T, Ortmann F, Meyer J C and Roche S 2013 Scaling properties of charge transport in polycrystalline graphene *Nano Lett.* **13** 1730
[37] Van Veldhoven Z A, Alexander-Webber J A, Sagade A A, Braeuninger-Weimer P and Hofmann S 2016 Electronic properties of CVD graphene: the role of grain boundaries, atmospheric doping, and encapsulation by ALD *Phys. Status Solidi* b **253** 2321
[38] Kang J H, Moon J, Kim D J, Kim Y, Jo I, Jeon C, Lee J and Hong B H 2016 Strain relaxation of graphene layers by Cu surface roughening *Nano Lett.* **16** 5993
[39] Kim Y-J, Kim Y, Novoselov K and Hong B H 2015 Engineering electrical properties of graphene: chemical approaches *2D Mater.* **2** 042001
[40] Kang J, Kim D, Kim Y, Choi J-B, Hong B H and Kim S W 2017 High-performance near-field electromagnetic wave attenuation in ultra-thin and transparent graphene films *2D Mater.* **4** 025003
[41] Kang S, Choi H, Lee S B, Park S C, Park J B, Lee S, Kim Y and Hong B H 2017 Efficient heat generation in large-area graphene films by electromagnetic wave absorption *2D Mater.* **4** 025037
[42] Lee Y, Bae S, Jang H, Jang S, Zhu S-E, Sim S-H, Song Y-I, Hong B H and Ahn J H 2010 Wafer-scale synthesis and transfer of graphene films *Nano Lett.* **10** 490–3
[43] Kang J, Kim H, Kim K S, Lee S K, Bae S, Ahn J H, Kim Y J, Choi J B and Hong B H 2011 High-performance graphene-based transparent flexible heaters *Nano Lett.* **11** 5154–8
[44] Han T-H, Lee Y, Choi M-R, Woo S-H, Bae S-H, Hong B H, Ahn J-H and Lee T-W 2012 Extremely efficient flexible organic light-emitting diodes with modified graphene anode *Nat. Photon.* **6** 105–10
[45] Bae S, Kim S J, Shin D, Ahn J H and Hong B H 2012 Towards industrial applications of graphene electrodes *Phys. Scr.* **2012** 014024